Mechanical Properties of Fibers Coated by Atomic Layer Deposition for Polymer-Matrix Composites with Enhanced Thermal and Ultraviolet Resistance



Robin E. Rodríguez, Tae H. Cho, M. Ravandi, William S. LePage, Mihaela Banu, M. D. Thouless and Neil P. Dasgupta

Abstract Interfacial engineering of fiber-reinforced composites is critical to control material properties, such as mechanical strength and toughness. In this study, we utilize atomic layer deposition (ALD) as a method to conformally coat structural fiber surfaces and study the impact of these interlayers on their mechanical adhesion to polymer-matrix materials. ALD of Al₂O₃, ZnO, and TiO₂ were applied to Kevlar[®] and carbon fibers, and microbond testing was performed using droplets of PMMA and Epoxy. It was observed that the mechanical force required for debonding of the polymer droplet from the coated fiber surfaces depended on the composition and thickness of the coating. Post-mortem scanning electron microscopy and energy dispersive X-ray spectroscopy for elemental analysis indicated that the ALD films remained adhered to the droplet, suggesting that the ALD/fiber interface limited the mechanical properties of the interphase region. Additionally, ALD of ZnO was demonstrated to prevent fiber degradation from ultraviolet (UV) and high-temperature thermal treatments, demonstrating a pathway towards multi-functional composite interphase engineering by ALD.

Keywords Atomic layer deposition \cdot Composite \cdot Fiber \cdot Polymer \cdot Sizing \cdot Coating \cdot Interface

Department of Materials Science and Engineering, University of Michigan, Ann Arbor, MI 48109, USA

R. E. Rodríguez · T. H. Cho · M. Ravandi · W. S. LePage · M. Banu · M. D. Thouless ·

N. P. Dasgupta (⊠)

Department of Mechanical Engineering, University of Michigan, Ann Arbor, MI 48109, USA e-mail: ndasgupt@umich.edu

Introduction

Fiber-reinforced composites (FRCs) have a high specific strength, stiffness, and toughness, and their use in vehicle systems offers improvements in performance and fuel efficiency. Further research and development of these low-density materials will enable transformational levels of performance for automotive and aerospace vehicles. A key area of research for the development of high-performance FRCs lies in the study of mechanical properties at the fiber/matrix interface. The desired mechanical properties of this interface vary for different types of FRCs. For fiber-reinforced polymer-matrix composites (PMCs), strong fiber/polymer interfaces are required to maximize load transfer to the fiber, as the polymer-matrix has relatively low stiffness and strength. In contrast, for fiber-reinforced ceramic-matrix composites (CMCs), weaker interfaces are generally desired. Typical ceramic matrices (e.g. silicon carbide, SiC) are relatively stiff and strong, but brittle. Therefore, fibers are added to increase toughness by providing a weak fiber/matrix interface that promotes crack deflection and dissipates energy [1, 2]. Thus, as the desired interfacial properties vary among composite material systems, new pathways to precisely modify the fiber/matrix interface would present opportunities for rational design of material properties of FRCs.

One way to modify the fiber/matrix interface is by coating the fiber surfaces before incorporating them into the matrix. Sizing layers are frequently added to fibers for protection during manufacturing, which may also be used to enhance the mechanical performance of a composite [3]. Sizings influence the strength and toughness at the fiber/matrix interface, which can be modified by changing the surface chemistry or morphology [4–7]. For example, previous surface modification of fibers has explored the addition of graphene oxide sheets [8] or carbon nanotubes (CNTs) to fiber surfaces [9, 10] to strengthen the interface of PMCs. Chemical vapor deposition (CVD) [10, 11] has also been used to coat glass fibers and carbon fibers. However, in the case of both PMCs and CMCs, the ability to conformally coat tows and woven fabrics is challenging due to high aspect-ratios and overlapping geometries that block line-ofsight deposition. As a result, these modified coating processes are often studied at the single-fiber level. CVD and physical vapor deposition (PVD) have been explored for coating fabrics; however, precise control of the composition and phase of the coatings on 3D templates can be challenging [12]. Furthermore, in the case of nanocomposites, the need for highly conformal and uniform deposition processes at the nanoscale is pivotal to engineer interfacial properties. This highlights the need for deposition processes that allow for precise control and tunability of process parameters.

Atomic layer deposition (ALD) is a gas-phase deposition technique that allows for improved conformality and precise compositional control compared to conventional gas-phase and solution-based processes [13]. It has been previously shown that ALD can conformally coat tows of fibers and woven fabrics, alleviating the limitations of other coating techniques [14–18]. Additionally, Liang et al. demonstrated that the mechanical properties of multi-wall carbon nanotubes (MWCNTs) dispersed in a polymer-derived ceramic matrix could be altered significantly by controlling the

coating material and the number of deposition cycles [19]. However, despite the advantages of ALD for interfacial engineering of composites, relatively few studies have explored the impact of ALD coatings on interfacial mechanics of FRCs [20].

In addition to modification of the mechanical properties of FRCs, interfacial coatings may also be used to introduce new functionality into the composite. For example, deposition of dispersed CNTs onto fiber surfaces has been shown to significantly change the electrical and thermal properties of a fiber-reinforced laminate [9, 10, 21]. PZT (PbZr $_{0.52}$ Ti $_{0.48}$ O $_3$) coatings on carbon fibers and BaTiO $_3$ coatings on SiC fibers have demonstrated that piezoelectric interfaces can be used to convert mechanical stress from vibrational energy into an electrical signal [22, 23]. These examples demonstrate that precisely engineered modifications at the interface of a FRC can enable the development of multi-functional composites.

Among the various modification methods available, ALD presents an excellent opportunity to develop multi-functional materials [24]. ALD can be used to deposit a wide range of material systems facilitating a virtually limitless selection and combination of materials with specific properties [25]. This ability to precisely tune interfacial chemistry and structure offers a powerful method for multi-functional composites development by design [26].

In this work, we performed single-fiber microbond tests to study the mechanical properties of the interface of two fiber-polymer material systems: carbon fiber/epoxy and Kevlar®/poly(methyl methacrylate). Aluminum oxide (Al₂O₃), titanium oxide (TiO₂), and zinc oxide (ZnO) coatings by ALD were used to study the effects of ALD modification on the mechanical properties at the interface. Furthermore, we demonstrate that ALD coatings can impart additional benefits, such as protection from radiation and thermal damage [28]. This added capability serves as a proof-of-concept demonstration that the development of multi-functional composites via ALD surface modification is possible.

Experimental Methods

The experimental procedure involved preparing samples for mechanical experiments (section "Material Systems and Specimen Preparation"). These mechanical experiments primarily used the microbond method (section "Microbond Test Setup and Procedure"), and single-fiber tensile tests were also performed to assess fiber degradation during UV and thermal exposure (section "Single-Fiber Tensile Tests of Kevlar® Fibers Exposed to Ultraviolet Radiation and Elevated Temperatures").

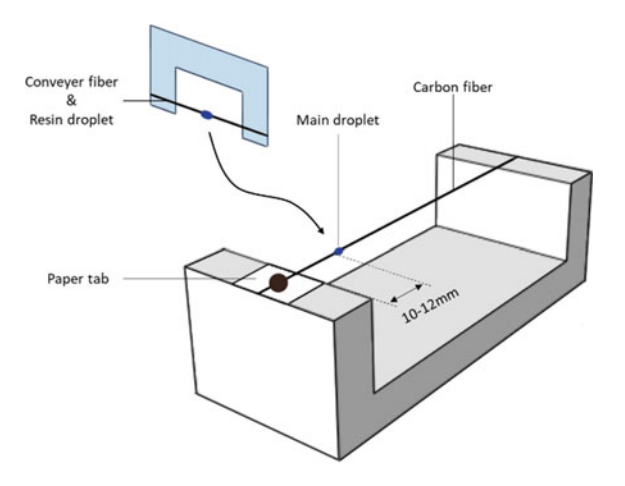
Material Systems and Specimen Preparation

Carbon Fiber/Epoxy

For the carbon fiber/epoxy material system, unsized HexTow® IM-8 carbon fibers (Hexcel Corporation; average fiber diameter of $5.2~\mu m$) were used with EPO-TEK® 301 thermoset polymer (Epoxy Technology, Inc.). Single carbon fibers were separated and cleaned by soaking in a boiling acetone bath for 10 min, followed by a boiling ethanol bath for 10 min, to remove any organics and contaminants from the fiber surface. The fibers were then rinsed in DI water for 5 min and dried in a vacuum oven at 130 °C for 3 h.

For the single-fiber microbond experiments, microdroplets of the polymermatrices (PMMA and epoxy) were added to the fibers. After cleaning and drying, the fibers were mounted horizontally on a custom frame and glued to a paper tab on one end of the fiber (Fig. 1). The paper tabs facilitated the handling of the fibers and helped prevent slippage when mounting the samples on the grips of the tensile stage. The uncured polymer droplets were produced by mixing 1 g of hardener for every 4 g of resin. The uncured epoxy microdroplets were transferred onto carbon fibers by means of a fiber-to-fiber resin transfer technique using a "conveyer fiber" (Fig. 1). A micro-pipet was used to add a droplet of resin on the conveyer fiber mounted on a paper frame. Next, the fiber was used to transfer the resin to the original specimen by bringing the fibers into perpendicular contact. The epoxy droplets were cured in a convection oven at 50 °C for 8 h and post-cured at room temperature for another 24 h. The droplets were observed in order to confirm that a symmetric geometry was obtained after curing, and the embedded lengths of the droplets were measured using an optical microscope. This technique produced consistent droplets with embedded lengths (L_{emb}) below 80 μ m. Droplets that exceeded this L_{emb} threshold required

Fig. 1 A conveyer fiber was used to place the epoxy droplet onto the sample fibers, which were mounted on a custom frame with a paper tab attached at one end



shear forces to debond the interface that exceeded the ultimate tensile strength of the carbon fiber.

Kevlar®/PMMA

Unsized single Kevlar[®] 351 para-aramid fibers (JPS Composite Materials; average fiber diameter of 12.6 µm) were extracted, cleaned, and mounted horizontally onto a frame with paper tabs at the end, in the same manner as the carbon fibers. Polymethyl methacrylate (PMMA) thermoplastic, with an average molecular weight of 120,000 by gel permeation chromatography (GPC), was used as the embedding microdroplet in this material system. A 3% wt PMMA solution was made by fully dissolving the PMMA powder in chloroform while stirring and heating to 70 °C for 10 min. After fully dissolving the PMMA, a droplet was placed on the Kevlar® fibers using the same fiber-to-fiber transfer technique. The chloroform solvent evaporates as soon as a drop is placed on the fiber, and the solidified PMMA does not immediately take the shape of an axisymmetric droplet. Therefore, the samples were heated to 200 °C for 2 h to allow the PMMA to melt and form into the desired droplet shape. Because the amount of polymer placed cannot be precisely controlled, some excess of PMMA may extend past the end of the droplet, forming a thin wetting layer. To remove this wetting layer, the fiber samples were submerged in chloroform for 3 min. This allowed the wetting layer to be fully etched without dissolving the PMMA droplet. The samples were then reheated to 200 °C for 1 h, and the final PMMA droplet shape was obtained. Droplets with embedded lengths greater than 250 µm resulted in the Kevlar® fibers breaking.

ALD Process

A custom-built, hot-wall, cross-flow thermal atomic layer deposition (ALD) reactor [28] was used for all ALD processes. Argon was used as the carrier gas for all ALD processes and was set with a flow rate of 70 sccm. For ALD of Al_2O_3 , the ALD reaction chamber was heated to 130 °C, and the trimethylaluminum (TMA, Sigma-Aldrich) and water precursors were evaporated from stainless steel cylinders at room temperature. An ALD cycle for depositing Al_2O_3 films consisted of a 0.05 s pulse TMA followed by a 30 s argon purge and then followed by a 0.1 s pulse of water and 30 s more of argon purging. The average growth rate of Al_2O_3 on a Si wafer under these conditions was measured to be 1.31 Å/cycle using spectroscopic ellipsometry.

For ALD of ZnO, the precursor and chamber temperature, the flow rate of the carrier gas, and the precursor pulse times were the same as those used for Al₂O₃. Diethylzinc (DEZ, Sigma-Aldrich) was used as the precursor. The growth rate of ZnO was measured to be 1.69 Å/cycle. The chamber temperature was 150 °C for the TiO₂ ALD processes. The carrier flow rates and precursor pulse times were the same as the previous two ALD processes. The tetrakis(dimethylamido)titanium (TDMAT, Sigma-Aldrich) precursor used for TiO₂ was heated to 75 °C. The growth rate for

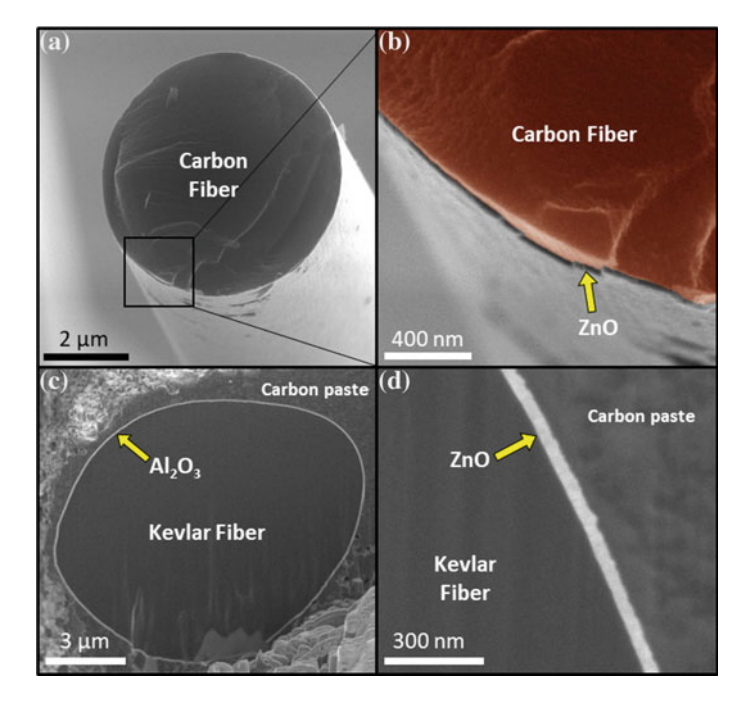


Fig. 2 a Low magnification and b high magnification SEM images of a carbon fiber coated with 20 nm of ZnO. c Low magnification SEM image of a Kevlar fiber with 50 nm of Al $_2$ O $_3$ and d high magnification SEM images of Kevlar fiber coated with 50 nm of ZnO. All images show conformal coverage of the ALD coatings

 TiO_2 was measured to be 0.74 Å/cycle. The Kevlar® fibers and carbon fibers were coated after drying in the convection oven (during the cleaning process) and before placing the polymer droplets on the fiber surfaces. The ALD coatings conformally coated both carbon fibers and Kevlar® fibers (Fig. 2), demonstrating the power of this technique for interfacial engineering of FRCs.

Microbond Test Setup and Procedure

The microbond test method was used to quantify the interfacial mechanical properties between a structural fiber and a polymer-matrix [29–31]. The method consisted of a micro-scale, axisymmetric polymer droplet that was placed on a single fiber, and then debonded by applying a shear force at the interface of the fiber/polymer (Fig. 3a). This is an alternative procedure to the single-fiber pull-out test [32–34], where very small embedded lengths (often in the micron scale) are necessary to avoid exceeding the ultimate strength of the fiber. The embedded length was defined as the geometrical length of the resin in the axial direction of the fiber, and the fiber/polymer interface

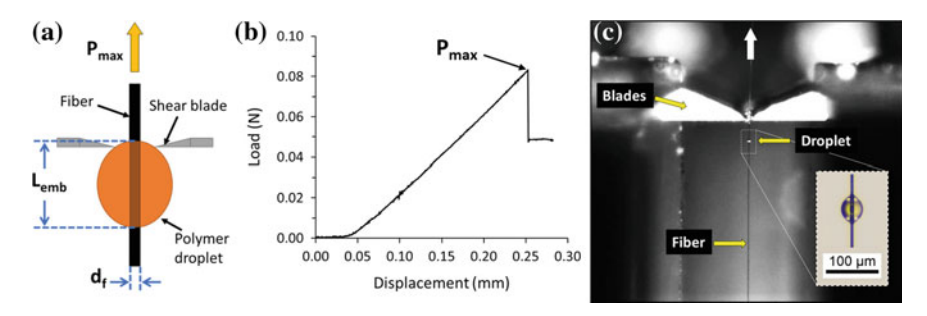


Fig. 3 a Schematic of the microbond method. b Representative load-displacement curve of a microbond test. c Image of an actual carbon fiber/epoxy sample mounted on the microvise, with shear blades in position and ready to be tested

area (A_{int}) is calculated as:

$$A_{\rm int} = \pi d_f L_{\rm emb}$$

where d_f is the nominal diameter of the structural fiber and $L_{\rm emb}$ is the embedded length.

The interfacial mechanical properties were calculated from the interfacial area and the peak load at debonding (Fig. 3b). A customized microvise setup, with position-adjustable shear blades, was designed and constructed to apply the shear load (Fig. 3c).

The microbond test was performed with the custom microvise on an Instron 3345 universal testing machine equipped with a 10 N load cell. The paper tab region of the droplet/fiber specimen was clamped in the upper grip attached to the displacement crosshead. The shear blade gap was adjusted by first bringing the razor blades into contact with the fiber and then retracting and adjusting the blade positions a specified distance. The blades were retracted approximately 2 µm from the contact position of the carbon fibers and approximately 5 µm from the contact position of the Kevlar® fibers. Accounting for the micrometer resolution accuracy of 2 µm, the blade gap was approximately 6-8 μm for carbon fiber/epoxy specimens and 15-20 μm for Kevlar®/PMMA specimens. The fiber was then pulled at a crosshead displacement rate of 0.05 mm/min, and the load was measured until an abrupt drop in the load was observed, signaling debonding of the polymer droplet. The peak load at the point of debonding was recorded and used to quantify the strength of the interface. Postmortem analysis was performed using optical and/or electron microscopy to ensure that samples included in the data set failed at the interface and not due to cohesive fracture of the droplet.

It is common to report the interfacial shear strength as an average value under the assumption of a uniform shear distribution at the interface [35, 36]. However, it is known that the shear stress distribution of the fiber-polymer interface is nonuniform during a microbond test [31, 35, 37, 38]. To properly estimate the interfacial shear

strength, an understanding of shear stress distribution at the interface would be necessary, requiring additional and extensive modeling. Variables such as fiber geometry, droplet size, razor blade position, and plasticity are parameters that need to be taken into account [30, 31, 37, 39, 40], but these are often difficult to measure or control experimentally, requiring assumptions to be made that may introduce multi-variable uncertainties into the model. Therefore, in this work, the experimental data reported will not be referred to as an intrinsic mechanical property—instead, the data will be denoted as the "force to debond per unit interfacial area" ($P_{\rm max}/A_{\rm int}$).

Single-Fiber Tensile Tests of Kevlar[®] Fibers Exposed to Ultraviolet Radiation and Elevated Temperatures

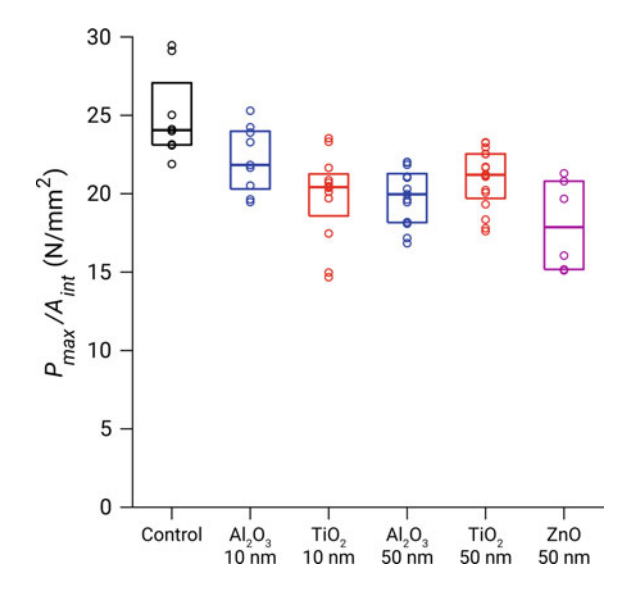
The protection capabilities of ZnO coatings in Kevlar® fibers against elevated temperature exposure and ultraviolet (UV) radiation were studied. Tensile tests were conducted to evaluate the effects of temperature and UV light on the ultimate tensile strength ($\sigma_{\rm ult}$) and work to failure (W_F) of the fibers. The Kevlar® fibers were cleaned by the same method in section "Carbon Fiber/Epoxy", and the ALD conditions for ZnO were similar to section "ALD Process", except the precursors that were exposed for a longer period. One cycle of this ALD recipe consisted of a DEZ pulse time/additional DEZ exposure time/Ar purge/H₂O pulse time/additional H₂O exposure time/Ar purge, of 0.05 s/10 s/30 s/0.10 s/10 s/30 s. The samples were then exposed to UV radiation (of an intensity of 15 W/m²) for 24 h or to temperatures of 300 °C for 8 h. The tensile properties of the Kevlar® fibers were tested using an RSA3 Dynamic Mechanical Analyzer (TA Instruments) following ASTM Standard C1557. The samples were pulled in tension at a constant displacement rate of 5 μ m/s until the fiber failed, and ultimate tensile strength ($\sigma_{\rm ult}$) and work to failure (W_F) were recorded.

Results and Discussion

Kevlar[®] Fiber and PMMA

The box plot in Fig. 4 shows the $P_{\rm max}/A_{\rm int}$ results for the Kevlar® fibers and PMMA. The average $P_{\rm max}/A_{\rm int}$ of uncoated Kevlar®/PMMA interfaces was 25.0 N/mm². The average $P_{\rm max}/A_{\rm int}$ of Kevlar®/PMMA interfaces with coatings of 10 nm Al₂O₃, 10 nm TiO₂, 50 nm Al₂O₃, 50 nm TiO₂, and 50 nm of ZnO was 22.2 N/mm², 19.8 N/mm², 19.8 N/mm², and 20.9 N/mm², and 18.0 N/mm², respectively. The 50 nm ZnO coated samples exhibited the weakest $P_{\rm max}/A_{\rm int}$ values with an average weakening of 28%, whereas the 10 nm Al₂O₃ coatings had the least detrimental effects on the interface, weakening the interface by an average of 11%. These results demonstrate

Fig. 4 Box plot of the force to debond per unit area of Kevlar®/PMMA samples with and without various ALD coatings



that ALD Al₂O₃, TiO₂, and ZnO coatings weaken the Kevlar[®]/PMMA interface, and the amount of weakening depends on both thickness and composition of the coating.

The results illustrate that nanometer-scale coatings of equal thickness, but different metal oxide composition, may result in significantly different interfacial mechanical properties. For example, the average $P_{\rm max}/A_{\rm int}$ for coatings of 50 nm thick TiO₂ was 6% greater than the 50 nm Al₂O₃ coated Kevlar[®], whereas fibers coated with 50 nm of ZnO were 11% weaker. Furthermore, the thickness of the ALD coatings also plays a role in influencing the mechanical properties at the interface. The average $P_{\rm max}/A_{\rm int}$ for 10 nm thick Al₂O₃ coatings was 12% stronger than the thicker 50 nm Al₂O₃ coatings. The opposite trend is observed for TiO₂, where the average $P_{\rm max}/A_{\rm int}$ for thinner 10 nm coatings was 5% weaker than the thicker 50 nm TiO₂ coatings. These results highlight the importance of the material and thickness control of the coatings on the interfacial mechanical properties of the Kevlar[®]/PMMA interface.

SEM analysis was used to inspect the samples after the microbond experiments, in order to observe the morphology of the polymer droplets after they debonded from the fiber. The PMMA droplets pulled off cleanly from the Kevlar® fibers with no traces of PMMA residue, for the entire set of Kevlar®/PMMA samples (including the coated samples). Interestingly, the ALD coatings were also observed to delaminate from the Kevlar® surface in the original region where the droplet was bonded to the fiber (Fig. 5). Both Al_2O_3 and ZnO coatings (50 nm thick) were absent in the original droplet position along the fiber surface after the microbond test (Fig. 5a, c, respectively). EDS elemental mapping further confirms the absence of Al_2O_3 and ZnO coatings in the debonding region (Fig. 5b, c, respectively).

These post-mortem observations suggest that the PMMA adheres more to the ALD coatings than the coatings adhere to the fiber. We therefore hypothesize that if the strength of adhesion between the ALD coatings and the Kevlar[®] fibers could

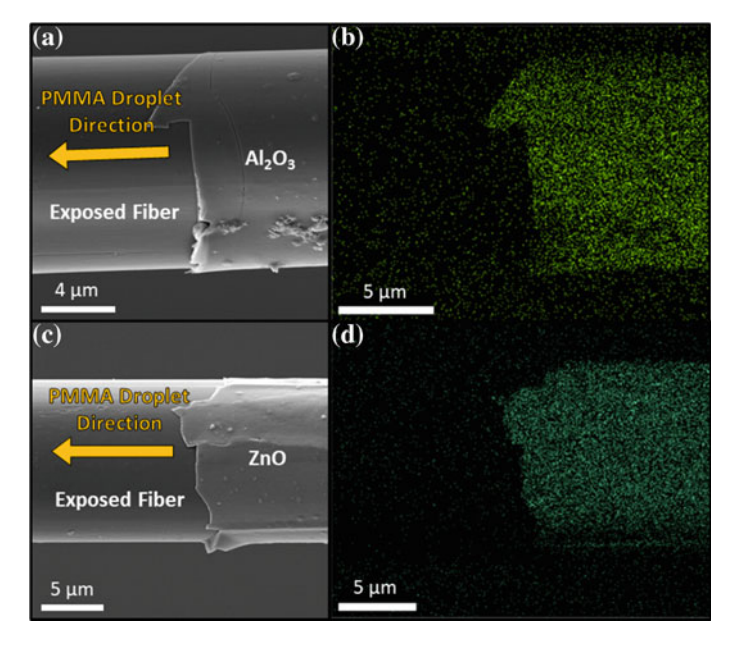


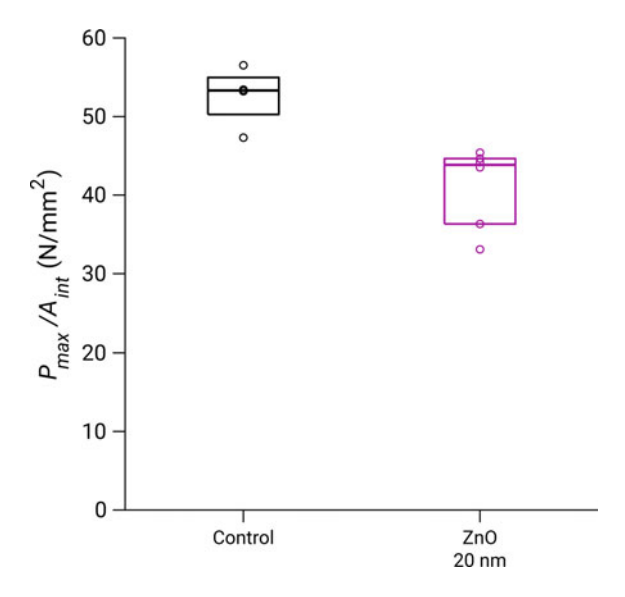
Fig. 5 a SEM image of a Kevlar®/50 nm Al_2O_3 /PMMA sample after the microbond test. The Al_2O_3 coating is not present where the PMMA droplet used to be as confirmed by **b** the EDS elemental map of Al. **c** SEM image of a Kevlar®/50 nm ZnO/PMMA sample after the microbond test. Similar to the Al_2O_3 sample, the ZnO coating is not present where the PMMA droplet used to be as confirmed by **d** the EDS elemental map of Zn

be enhanced, the $P_{\rm max}/A_{\rm int}$ could potentially reach or even surpass that of the bare Kevlar®/PMMA. Chen et al. [41] showed that the interfacial toughness was lower when delamination occurred at the ALD/polymer beam interface than when it occurred at the ALD/epoxy interface. This also indicates that control of the interface (fiber/ALD or ALD/epoxy) at which crack-propagation occurs can have a significant impact on debonding force. Future work dedicated to modification of the interfacial chemistry between ALD coatings and the Kevlar® fibers would help identify surface treatments that could promote stronger or weaker adhesion, depending on the targeted application.

Carbon Fiber and Epoxy

The $P_{\rm max}/A_{\rm int}$ was also evaluated for the material combination of carbon fiber and epoxy (Fig. 6). The average interfacial $P_{\rm max}/A_{\rm int}$ of bare and 20 nm ZnO coated carbon fibers with epoxy was 52.6 and 41.2 N/mm². Similar to the microbond results of the Kevlar®/PMMA material system, the average $P_{\rm max}/A_{\rm int}$ of the 20 nm ZnO coated carbon fibers/epoxy weakened by 21.7% as compared to the bare fibers/epoxy.

Fig. 6 Box plot of the force to debond per unit area of carbon fiber/epoxy samples with and without 20 nm ZnO coatings



These results demonstrate that ALD coatings can impact a range of fiber-matrix combinations, and provide motivation for a deeper understanding of the coupled chemical-mechanical properties of ALD-modified FRC interfaces.

Statistical Significance Analysis

Statistical analysis was conducted to confirm that ALD coatings have a measurable effect on the average weakening of the $P_{\rm max}/A_{\rm int}$. The statistical significance of the $P_{\rm max}/A_{\rm int}$ measurements for coated fibers was evaluated against the fibers without coatings, using a one-tailed t-test. The null hypothesis for this test is that ALD coatings on the fiber/polymer interface have no direct effect on the $P_{\rm max}/A_{\rm int}$ values obtained. The null hypothesis will be rejected if the p-value is less than 0.05 (confidence interval of 95%). The calculated p-values for each ALD coating and material system are listed in Table 1. The significance level criteria previously established are met for all coatings and material systems, and thus, the null hypothesis is fully rejected, supporting the conclusions that the ALD coatings can systematically modify interfacial mechanical properties.

Ultraviolet and Thermal Protection

In addition to modification of mechanical properties of fiber/matrix interfaces, coatings are often used on fiber surfaces to protect them during composite materials

1524 R. E. Rodríguez et al.

Table 1 *t*-test results of the statistical significance of the $P_{\text{max}}/A_{\text{int}}$ from Figs. 4 and 6

Coating	t-score	Degrees of freedom	<i>p</i> -value (<i>p</i> < 0.05)
Kevlar®/PMM	A		
10 nm Al ₂ O ₃	2.2840	15	0.0187
10 nm TiO ₂	4.0115	18	0.0004
50 nm Al ₂ O ₃	4.6399	22	0.0006
50 nm TiO ₂	3.6861	12	0.0004
50 nm ZnO	4.5141	19	0.0001
Carbon fiberle	роху		
20 nm ZnO	4.0030	8	0.0020

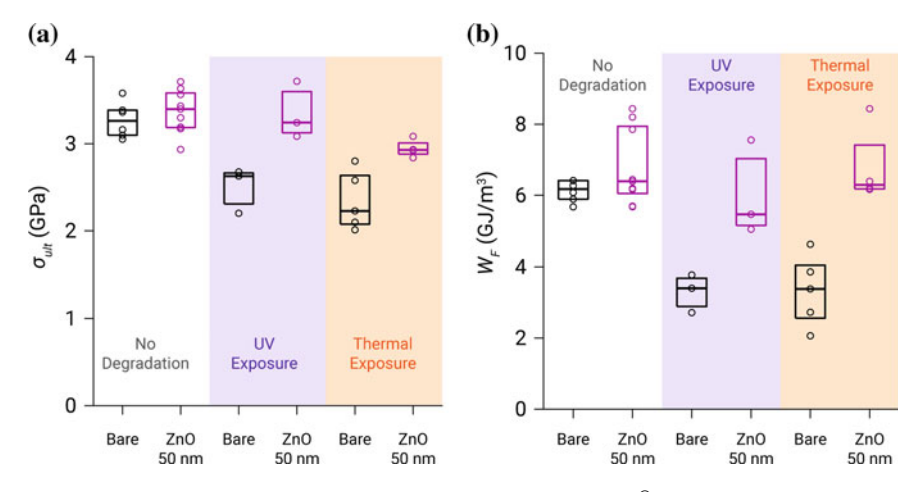


Fig. 7 a Ultimate tensile strength $\bf b$ and work to failure of the Kevlar[®] fibers exposed to ultraviolet radiation and 300 °C temperatures, with and without 50 nm ZnO coatings by VPI, were obtained

processing. Coatings may also be used to protect a composite from environmental conditions. Polymers often experience effects of degradation when exposed to extreme radiation or temperatures, which can often limit their use. Coatings that can protect a polymer-matrix or polymer fiber from these detrimental effects would enable the use of polymer composites in wider range of applications.

The ability of ALD ZnO coatings to protect Kevlar[®] fibers from ultraviolet (UV) radiation thermal degradation was evaluated by measuring the ultimate tensile strength ($\sigma_{\rm ult}$) and work to failure (W_F) of the fibers (Fig. 7). UV light exposure, of an intensity of 15 W/m² for 24 h, reduced the average $\sigma_{\rm ult}$ of uncoated fibers by 24% and the average W_F by 46%. Furthermore, uncoated fibers that were exposed to an ambient temperature of 300 °C for 8 h experienced a decrease in $\sigma_{\rm ult}$ by 30% and a decrease in W_F by 46% (Fig. 7). In contrast, Kevlar[®] fibers with a 50 nm coating of ZnO by ALD had a negligible change in the average $\sigma_{\rm ult}$ (0% difference) and the average W_F (2% lower) after the same UV treatment. Similarly, Kevlar[®] fibers

with the ZnO coatings reduced the impact of thermal degradation in the average $\sigma_{\rm ult}$ (12% weaker) and increased the average W_F (11% higher). It is also evident that the ZnO coatings did not influence the average $\sigma_{\rm ult}$ significantly (3% stronger), but did slightly increase the average W_F (11% higher). The UV protection capabilities shown here are consistent with previous work from Azpitarte et al. [27].

Conclusions

Understanding the interfacial properties is crucial to predict the overall mechanical properties of FRCs. The ability to tune the interfacial properties, not only in PMCs but also CMCs, presents an opportunity to develop engineered structural composite materials designed with specific macroscopic mechanical properties. In this study, we explored the effects ALD coatings have on the interface of two distinct fiber/polymer material systems. We demonstrated ALD can conformally coat Kevlar® fibers and carbon fibers with sub-nm thickness control, and that this level of thickness control can influence the interfacial properties of both material systems (Kevlar®/PMMA and carbon fiber/epoxy). Furthermore, we showed that the mechanical response of ALD coated fibers depends on coating thickness and composition. It was observed that the ALD coatings preferentially delaminated from Kevlar® fiber surfaces, indicating that the adhesion of the coatings to the matrix was higher than the adhesion of the coatings to the fiber surfaces. Finally, it was demonstrated that ALD coatings could be used to impart additional benefits beyond tuning interfacial bonding. As a proof-of-concept, we showed that deposition of 50 nm of ZnO by ALD can protect Kevlar® fibers from ultraviolet light degradation and thermal degradation. This model material system demonstrates that ALD coatings could enable opportunities to produce multi-functional composites, bringing forth an exciting new field of research and development.

Acknowledgements This work was supported by the Air Force Office of Scientific Research (AFOSR) under Grant FA9550-16-1-0313. This material is based upon work supported by the National Science Foundation under Grant No. 1751590. The authors acknowledge the financial support of the University of Michigan College of Engineering and NSF Grant #DMR-9871177 and technical support from the Michigan Center for Materials Characterization.

References

- Parmigiani JP, Thouless MD (2006) The roles of toughness and cohesive strength on crack deflection at interfaces. J Mech Phys Solids 54(2):266–287
- Martin E, Leguillon D, Lacroix C (2002) An energy criterion for the initiation of interface failure ahead of a matrix crack in brittle matrix composites. Compos Interfaces 9(2):143–156
- 3. Jones FR (2010) A review of interphase formation and design in fibre-reinforced composites. J Adhes Sci Technol 24(1):171–202

- 4. Dai Z, Shi F, Zhang B, Li M, Zhang Z (2011) Effect of sizing on carbon fiber surface properties and fibers/epoxy interfacial adhesion. Appl Surf Sci 257(15):6980–6985
- Berg J, Jones FR (1998) The role of sizing resins, coupling agents and their blends on the formation of the interphase in glass fibre composites. Compos Part A Appl Sci Manuf 29(9– 10):1261–1272
- Yuan H, Zhang S, Lu C, He S, An F (2013) Improved interfacial adhesion in carbon fiber/polyether sulfone composites through an organic solvent-free polyamic acid sizing. Appl Surf Sci 279:279–284
- Gnädinger F, Middendorf P, Fox B (2016) Interfacial shear strength studies of experimental carbon fibres, novel thermosetting polyurethane and epoxy matrices and bespoke sizing agents. Compos Sci Technol 133:104–110
- 8. Zhang X, Fan X, Yan C, Li H, Zhu Y, Li X, Yu L (2012) Interfacial microstructure and properties of carbon fiber composites modified with graphene oxide. ACS Appl Mater Interfaces 4(3):1543–1552
- Tamrakar S, An Q, Thostenson ET, Rider AN, Haque BZ, Gillespie JW (2016) Tailoring interfacial properties by controlling carbon nanotube coating thickness on glass fibers using electrophoretic deposition. ACS Appl Mater Interfaces 8(2):1501–1510
- Rider AN, An Q, Brack N, Thostenson ET (2016) A comparison of mechanical and electrical properties in hierarchical composites prepared using electrophoretic or chemical vapor deposition of carbon nanotubes. MRS Adv 1(12):785–790
- Qian H, Bismarck A, Greenhalgh ES, Kalinka G, Shaffer MSP (2008) Hierarchical composites reinforced with carbon nanotube grafted fibers: the potential assessed at the single fiber level. Chem Mater 20(5):1862–1869
- Mogilevsky P, Boakye EE, Key TS, Parthasarathy TA, Hay RS, Cinibulk MK (2019) In situ Y₂Si₂O₇ coatings on SiC fibers: thermodynamic analysis and processing. J Am Ceram Soc 102(1):167–177
- Dasgupta NP, Lee HBR, Bent SF, Weiss PS (2016) Recent advances in atomic layer deposition. Chem Mater 28(7):1943–1947
- Militzer C, Dill P, Goedel WA (2017) Atomic layer deposition onto carbon fiber fabrics. J Am Ceram Soc 100(12):5409–5420
- Daubert JS, Mundy JZ, Parsons GN (2016) Kevlar-based supercapacitor fibers with conformal pseudocapacitive metal oxide and metal formed by ALD. Adv Mater Interfaces 3(21):1600355
- 16. Gregorczyk KE, Pickup DF, Sanz MG, Irakulis IA, Rogero C, Knez M (2015) Tuning the tensile strength of cellulose through vapor-phase metalation. Chem Mater 27(1):181–188
- 17. Hyde GK, Scarel G, Spagnola JC, Peng Q, Lee K, Gong B, Roberts KG, Roth KM, Hanson CA, Devine CK, Stewart SM, Hojo D, Na JS, Jur JS, Parsons GN (2010) Atomic layer deposition and abrupt wetting transitions on nonwoven polypropylene and woven cotton fabrics. Langmuir 26(4):2550–2558
- 18. Jur JS, Spagnola JC, Lee K, Gong B, Peng Q, Parsons GN (2010) Temperature-dependent subsurface growth during atomic layer deposition on polypropylene and cellulose fibers. Langmuir 26(11):8239–8244
- 19. Liang X, Yang Y, Lou J, Sheldon BW (2017) The impact of core-shell nanotube structures on fracture in ceramic nanocomposites. Acta Mater 122:82–91
- Vogel S, Dransfeld C, Fiedler B, Gobrecht J, (2014) Protective effect of thin alumina layer on carbon fibre to preserve tensile strength during CNT growth by CVD. In: 16th European conference on composite. Materials. ECCM 2014, Seville, Spain, 22–26 June 2014
- Yamamoto N, Guzman de Villoria R, Wardle BL (2012) Electrical and thermal property enhancement of fiber-reinforced polymer laminate composites through controlled implementation of multi-walled carbon nanotubes. Compos Sci Technol 72(16):2009–2015
- Lin Y, Shaffer JW, Sodano HA (2010) Electrolytic deposition of PZT on carbon fibers for fabricating multifunctional composites. Smart Mater Struct 19(12):124004
- Lin Y, Sodano HA (2009) Fabrication and electromechanical characterization of a piezoelectric structural fiber for multifunctional composites. Adv Funct Mater 19(4):592–598

- Rodríguez RE, Agarwal SP, An S, Kazyak E, Das D, Shang W, Skye R, Deng T, Dasgupta NP (2018) Biotemplated morpho butterfly wings for tunable structurally colored photocatalysts. ACS Appl Mater Interfaces 10(5):4614–4621
- Miikkulainen V, Leskelä M, Ritala M, Puurunen RL (2013) Crystallinity of inorganic films grown by atomic layer deposition: overview and general trends. J Appl Phys 113(2):021301
- 26. Zeng L, Liu X, Chen X, Soutis C (2018) Surface modification of aramid fibres with graphene oxide for interface improvement in composites. Appl Compos Mater 25(4):843–852
- Azpitarte I, Zuzuarregui A, Ablat H, Ruiz-Rubio L, López-Ortega A, Elliott SD, Knez M (2017)
 Suppressing the thermal and ultraviolet sensitivity of kevlar by infiltration and hybridization with ZnO. Chem Mater 29(23):10068–10074
- Dasgupta NP, Mack JF, Langston MC, Bousetta A, Prinz FB (2010) Design of an atomic layer deposition reactor for hydrogen sulfide compatibility. Rev Sci Instrum 81(4):044102
- 29. Sockalingam S, Nilakantan G (2012) Fiber-matrix interface characterization through the microbond test: a review. Int J Aeronaut Sp Sci 13(3):282–295
- Nishikawa M, Okabe T, Hemmi K, Takeda N (2008) Micromechanical modeling of the microbond test to quantify the interfacial properties of fiber-reinforced composites. Int J Solids Struct 45(14–15):4098–4113
- 31. Miller B, Gaur U, Hirt DE (1991) Measurement and mechanical aspects of the microbond pull-out technique for obtaining fiber/resin interfacial shear strength. Compos Sci Technol 42(1–3):207–219
- 32. Meretz S, Nowak H, Hampe A, Hinrichsen G, Schumacher K, Sernow R (1991) Investigations of interfacial shear strength between reinforcing fibres and polymer matrix with the single fibre pull-out test. In: Second international conference of interfacial phenom. Composition materials, Leuven, Belgium, 17–19 Sept 1991, pp 73–76
- 33. Wu K, Xu Y, Cheng X (2018) Simulation and analysis of single fiber pull-out tests through ANSYS and VC++. Int J Adv Manuf Technol 96(5–8):1591–1599
- 34. Feih S, Schwartz P (1997) FEM analysis and comparison of single fiber pull-out tests. Adv Compos Lett 6(4):99–102
- 35. Kang SK, Lee DB, Choi NS (2009) Fiber/epoxy interfacial shear strength measured by the microdroplet test. Compos Sci Technol 69(2):245–251
- 36. Gu X, Young RJ (1997) Deformation micromechanics in model carbon fiber reinforced composites part II: the microbond test. Text Res J 67(2):93–100
- Day RJ, Cauich Rodrigez JV (1998) Investigation of the micromechanics of the microbond test. Compos Sci Technol 58(6):907–914
- 38. Zhandarov S, Mäder E (2013) Analysis of a pull-out test with real specimen geometry. Part I: matrix droplet in the shape of a spherical segment. J Adhes Sci Technol 27(4):430–465
- Zhao Q, Qian CC, Harper LT, Warrior NA (2018) Finite element study of the microdroplet test for interfacial shear strength: effects of geometric parameters for a carbon fibre/epoxy system. J Compos Mater 52(16):2163–2177
- Zhi C, Long H, Miao M (2017) Influence of microbond test parameters on interfacial shear strength of fiber reinforced polymer-matrix composites. Compos Part A Appl Sci Manuf 100:55-63
- 41. Chen Y, Ginga N, LePage WS, Kazyak E, Gayle A, Wang J, Rodríguez RE, Thouless MD, Dasgupta NP (Submitted) Enhanced interfacial toughness of thermoplastic-epoxy interfaces using ald surface treatments